PROCEEDINGS OF SCIENCE

PoS(EPS-HEP2025)418

ATL-PHYS-PROC-2025-126
08 December 2025

# Searches for new phenomena in hadronic final states using the ATLAS detector

**Marawan Barakat**[a,*] **on behalf of the ATLAS Collaboration**

[a] *DESY, Zeuthen, Germany*

*E-mail:* marawan.barakat@cern.ch

Many theories beyond the Standard Model predict new phenomena giving rise to multijet final states. These jets can originate from the decay of heavy resonances into Standard Model quarks or gluons, or from more complex decay chains involving dark-sector particles. Also of interest are resonant and non-resonant hadronic final states where jets stem from a dark sector, leading to a diverse phenomenology depending on the interactions between dark and visible particles. This contribution summarises recent ATLAS results based on 13 TeV Run 2 data, highlighting three complementary analyses targeting boosted light resonances, flavour-violating dark matter, and semi-visible jets.

*The European Physical Society Conference on High Energy Physics (EPS-HEP 2025)*
*6–11 July 2025, Marseille, France*

[*] Speaker


ISSN 1824-8039. Published by SISSA Medialab.

## 1. Introduction

Hadronic final states are a cornerstone of searches for new particles at the Large Hadron Collider (LHC) [1]. The strong coupling of many hypothetical beyond Standard Model (BSM) particles to quarks and gluons offers exceptional sensitivity to a broad range of models. Depending on the mediator mass (the mass of the exchanged BSM particle) and coupling structure, such signatures can appear as narrow dijet resonances, multi-jet cascades, or as topologies containing significant missing transverse momentum ($E_{\mathrm{T}}^{\mathrm{miss}}$) from invisible particles.

The ATLAS detector [2] recorded the full Run 2 dataset of proton–proton collisions at $\sqrt{s}$ = 13 TeV. The following sections summarise three representative ATLAS analyses exploring hadronic final states from complementary perspectives:

1. A search for boosted low-mass resonances recoiling against an initial-state photon [7].
2. A reinterpretation of a flavour-violating supersymmetry (SUSY) search in terms of dark-matter-flavour-violation (DMFV) models [8].
3. A search for semi-visible jets and anomalous hadronic signatures that employs advanced machine-learning (ML) techniques [10].

Together, these analyses illustrate how ATLAS hadronic searches combine traditional cut-based strategies with modern, data-driven frameworks capable of identifying targeted phenomena.

## 2. ATLAS detector and event reconstruction

The ATLAS detector [2] is a multipurpose apparatus with nearly $4\pi$ coverage in solid angle, designed to measure the trajectories and energies of particles produced in proton–proton collisions at the LHC. Jets are reconstructed from topological calorimeter clusters using the anti-$k_t$ algorithm with radius parameters $R = 0.4$ and $R = 1.0$ for small- and large-$R$ jets, respectively. The missing transverse momentum, $E_{\mathrm{T}}^{\mathrm{miss}}$ [11], is calculated as the magnitude of the negative vector sum of the transverse momenta of all calibrated reconstructed objects, using only small-$R$ jets for the jet term and excluding large-$R$ jets, supplemented by tracks from the primary vertex that are not associated to identified objects. Heavy-flavour jets are identified using dedicated $b$- and $c$-tagging algorithms [3], while large-$R$ jet substructure and grooming techniques [4] improve the reconstruction of boosted hadronic decays. In the analyses reported in this document, events are recorded using a combination of photon, jet, and $E_{\mathrm{T}}^{\mathrm{miss}}$ triggers, selected to ensure full efficiency for each of the signal topologies discussed in the following sections.

## 3. Boosted low-mass resonances with an ISR photon

**Motivation and model** $Z'$ mediators arise in many dark matter models [5, 6], corresponding to a light spin-1 mediator that couples to SM quarks and the dark sector. In the 20–100 GeV mass range, dijet triggers are limited by the high QCD multijet rate. Selecting an energetic photon from initial-state radiation (ISR) enables the topology $q\bar{q} \to \gamma Z' \to \gamma q\bar{q}$, where the $Z'$ is boosted and its hadronic decay forms a single large-$R$ jet.

**Event selection and background** Events are required to contain a photon with $p_{\mathrm{T}} > 150$ GeV and a large-$R$ jet with $p_{\mathrm{T}} > 150$ GeV and $|\eta| < 2.0$, separated by $\Delta R > 0.4$. A two-prong substructure tagger $D^2_{\mathrm{DDT}}$ is used to distinguish signal-like from QCD jets. Tagged ($D^2_{\mathrm{DDT}} < 0$) and anti-tagged ($D^2_{\mathrm{DDT}} > 0$) regions are combined with photon centrality categories to define control regions for background processes. Multijet backgrounds with mis-identified photons are reduced using tight photon identification and isolation.

**Results** The large-$R$ jet mass $m_J$ is used as the search observable. No significant excess is observed (Figure 1). Upper limits are set on the quark–$Z'$ coupling $g_q$ versus $m_{Z'}$. Mediators with $g_q = 0.2$ are excluded up to $m_{Z'} \approx 80$ GeV, extending ATLAS sensitivity well below the traditional dijet threshold, in a mass range hitherto unprobed by the ATLAS Collaboration.

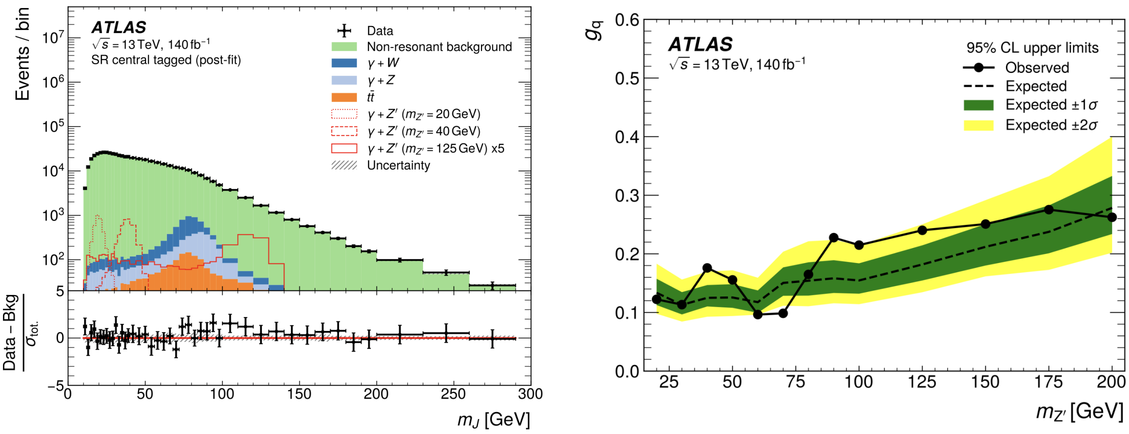


**Figure 1: Left:** Post-fit $m_J$ spectrum in the central tagged signal region, with background prediction and benchmark $\gamma + Z'$ signals. **Right:** 95% CL upper limits on the quark coupling $g_q$ as a function of $m_{Z'}$, with $\pm 1\sigma$ and $\pm 2\sigma$ expected bands [7].

## 4. Dark-Matter Flavour-Violation reinterpretation

**Signal Framework** DMFV is a framework in which the dark sector contains three flavours of fermionic dark matter (DM), usually denoted $\chi_{1,2,3}$, that transform in analogy with the three generations of quarks. These dark flavours interact with the Standard Model through a new coloured scalar mediator $\phi$ that carries the gauge quantum numbers of an up-type quark. The interaction between quarks and dark matter is controlled by a complex coupling matrix, often referred to as $\lambda$, which is the single new source of flavour violation in the theory. DMFV models are built to satisfy constraints from direct detection, flavour physics, and cosmology, ensuring that the three dark flavours and their couplings yield a viable relic abundance.

**Analysis strategy** The study reuses an ATLAS search for flavour-violating SUSY stops, $\tilde{t}_1\tilde{t}_1^* \to t\,c + \tilde{\chi}_1^0\tilde{\chi}_1^0$, which yields the same final state as $\phi\phi^\dagger \to t\,\bar{c} + \chi\bar{\chi}$. Events must satisfy $E_{\mathrm{T}}^{\mathrm{miss}} > 250$ GeV, contain at least one $b$- and one $c$-tagged jet, and obey $\min\Delta\phi(E_{\mathrm{T}}^{\mathrm{miss}}, j_{1,2,3,4}) > 0.4$. Boosted tops are reconstructed using large-$R$ jets and a dedicated neural-network tagger. Four signal regions target different $\Delta m(\phi, \chi)$ regimes using sensitive variables such as the stransverse mass [9]

$m_{T2}(j_b^{R=1.0}, j_c)$, built between the top-tagged large-$R$ jet and the charm-tagged jet, the transverse mass between $E_{\mathrm{T}}^{\mathrm{miss}}$ and the jet closest to it $m_{\mathrm{T}}(j, E_{\mathrm{T}}^{\mathrm{miss}})_{\mathrm{close}}$, and the effective mass of the event $m_{\mathrm{eff}}$. Control regions normalise $Z$+jets, single-top, and $t\bar{t}$ backgrounds.

**Results and interpretation** A global likelihood fit including all signal and control regions yields no deviation from the Standard Model. Figure 2 shows the resulting 95 % CL limits. For the right-handed single-flavour freeze-out benchmark, mediator masses up to about 1.2 TeV are excluded for large $D_{\lambda,11} \approx 2$. The reinterpretation provides the first collider constraints linking top-charm flavour violation with a dark sector, demonstrating the synergy between SUSY and DM frameworks.

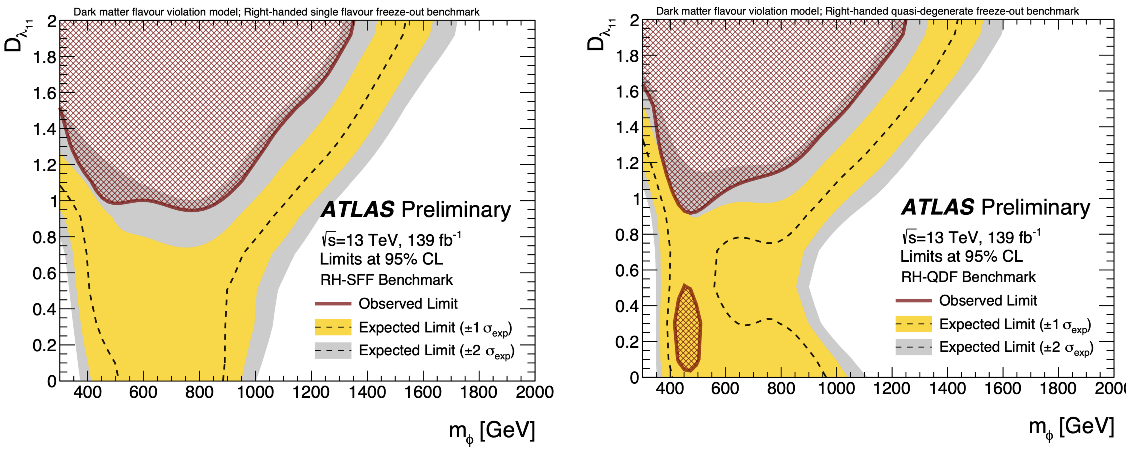


**Figure 2:** Observed and expected 95% CL exclusions in the plane of the mediator mass $m_\phi$ and the coupling $D_{\lambda,11}$ for two right-handed DMFV benchmarks: **Left**: single-flavour freeze-out (RH-SFF). **Right**: quasi-degenerate freeze-out (RH-QDF) [8].

## 5. Semi-visible jets and anomaly-sensitive selections

**Signal concept** Hidden-valley models [14, 15] with a confining dark gauge group $SU(N_D)$ predict dark quarks that hadronise into dark mesons. A heavy mediator $Z'$ produced in the $s$-channel can decay into these dark quarks, $pp \to Z' \to \chi_D \bar{\chi}_D$, each forming a semi-visible jet (SVJ) composed of both visible and invisible constituents. The fraction of invisible energy $R_{\mathrm{inv}}$ determines the degree of alignment between the jets and $E_{\mathrm{T}}^{\mathrm{miss}}$. Unlike typical QCD jets, SVJs exhibit a high charged-particle multiplicity, a large spread in the transverse momentum of constituents, and a correlation between the $E_{\mathrm{T}}^{\mathrm{miss}}$ direction and the jet axis.

**Event selection** Events with at least two small-$R$ jets ($p_{\mathrm{T}} > 150$ GeV, $|\eta| < 2.1$) and $E_{\mathrm{T}}^{\mathrm{miss}} > 200$ GeV are selected, with $\Delta\phi(j_1, j_2) > 0.8$ and $|\Delta y(j_1, j_2)| < 2.8$. The $E_{\mathrm{T}}^{\mathrm{miss}}$ trigger and offline thresholds ensure high efficiency across the entire signal region. The search is split into two orthogonal machine-learning regions targeting complementary aspects of the event topology.

**Particle-Flow Network (PFN)** The PFN [12] is a permutation- and variable-length–invariant architecture designed to operate directly on the set of reconstructed particle-flow candidates. Each constituent $i$ is represented by a six-dimensional feature vector $(p_T, \eta, \phi, E, d_0, z_0)$. An embedding

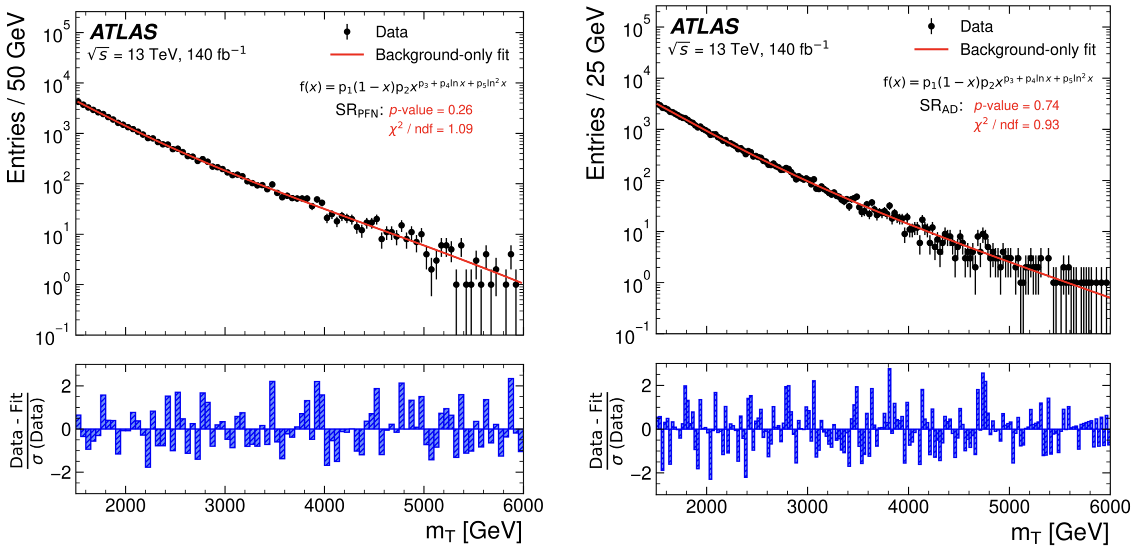


**Figure 3:** Transverse mass spectra in the semi-visible jet search. **Left:** SR$_{\mathrm{PFN}}$ using the supervised Particle-Flow Network classifier. **Right:** SR$_{\mathrm{AD}}$ using the semi-supervised ANTELOPE anomaly detector. Both regions show good agreement between data and the background-only fit [10].

network maps each particle to a latent representation $\Phi(x_i)$; the latent vectors are then summed, preserving permutation invariance, and passed to a fully connected classifier. The network is trained using labelled Monte Carlo samples of SVJ signal and multijet background, optimising a binary cross-entropy loss. Training is performed on events with balanced classes, and the model is regularised via dropout and early stopping. The output score score$_{\mathrm{PFN}}$, reflects the probability of an event being signal-like. Events with score$_{\mathrm{PFN}} > 0.6$ define SR$_{\mathrm{PFN}}$, a signal region targeting the SVJ model with a PFN-based approach. This supervised approach achieves strong discrimination, with an area under the ROC curve of approximately 0.93. The PFN captures subtle correlations among track-based variables that are difficult to encode with conventional jet substructure observables.

**ANTELOPE anomaly detection** To complement the supervised training, a semi-supervised model named ANTELOPE (*Anomaly-TEsted Latent Outlier Probabilistic Encoder*) [13] is employed. It is built as a variational autoencoder (VAE) trained exclusively on background-dominated data, using the same PFN input representation. The encoder compresses each event into a latent space while the decoder attempts to reconstruct the original input. During training, the loss function combines the reconstruction error and the Kullback–Leibler divergence between the latent distribution and a unit Gaussian prior. The anomaly score is defined as the negative log-likelihood of the reconstruction, providing a measure of deviation from the learned background manifold. Events with an anomaly score above the 90$^{\mathrm{th}}$ percentile of the background distribution populate SR$_{\mathrm{AD}}$, a signal region defined using the anomaly-detection score for model-independent searches. This data-driven method enables sensitivity to a wide variety of unforeseen BSM signatures, including long-lived particles, emerging jets, or heavy-flavour–enriched dark showers.

**Validation and systematics** Both models are validated in independent control regions dominated by QCD multijets. The stability of the PFN and ANTELOPE outputs is verified against variations in jet energy scale and resolution, pile-up conditions, and trigger efficiency. The observed agreement between data and simulation in the sidebands confirms that the models do not introduce spurious sculpting in kinematic variables such as $m_T$ or $E_{\mathrm{T}}^{\mathrm{miss}}$. Systematic uncertainties in the fit include variations of jet calibration, track reconstruction efficiency, and the modelling of the analytic background shape. The impact of these uncertainties on the extracted limits is below 10% for most of the parameter space.

**Results** The transverse mass $m_T(j_1, j_2, E_{\mathrm{T}}^{\mathrm{miss}})$ spectra in $\mathrm{SR_{PFN}}$ and $\mathrm{SR_{AD}}$ are shown in Figure 3. No significant excess is observed; background-only fits yield $p$-values of 0.26 and 0.74 respectively. Upper limits on the signal production cross section times branching ratio are set at 95% confidence level using the $CL_s$ method. As the data show no significant excess over the background expectation, the observed and expected limits agree well. Signal points with $m_{Z'}$ between 2.0 and 3.2 TeV are excluded for $R_{\mathrm{inv}}$ values in the range 0.2–0.37. The combination of PFN and ANTELOPE provides a powerful demonstration of how deep-learning architectures and data-driven anomaly detection can jointly extend the discovery reach of hadronic searches beyond the boundaries of explicit model hypotheses.

## 6. Conclusion

Hadronic final states continue to be a powerful probe of new physics at the LHC. The three analyses presented here exploit complementary signatures and analysis techniques: a dijet + ISR photon signature that opens sensitivity to light resonances beyond standard dijet searches, a reinterpretation connects flavour-violating SUSY and dark-sector flavour violating models and machine-learning-driven selections extend discovery reach to semi-visible jets topologies. No significant deviations from the Standard Model have been observed so far. The growing Run 3 dataset and improved substructure and ML techniques will further enhance ATLAS sensitivity to new phenomena in hadronic final states.

## References

[1] L. Evans and P. Bryant, “LHC Machine”, *JINST* **3** (2008) S08001.

[2] ATLAS Collaboration, “The ATLAS Experiment at the CERN Large Hadron Collider”, *JINST* **3** (2008) S08003.

[3] ATLAS Collaboration, “Optimisation and performance of the ATLAS $b$-tagging algorithms for Run 2”, ATL-PHYS-PUB-2017-013 (2017).

[4] ATLAS Collaboration, “Jet substructure performance for large-$R$ jets in ATLAS”, ATL-PHYS-PUB-2021-011 (2021).

[5] D. Abercrombie *et al.*, “Dark Matter benchmark models for early LHC Run-2 searches: Report of the ATLAS/CMS Dark Matter Forum”, *Phys. Dark Univ.* **27** (2020) 100371.

[6] A. Boveia *et al.*, “Recommendations on presenting LHC searches for missing transverse energy signals using simplified $s$-channel models of dark matter”, (no journal published).

[7] ATLAS Collaboration, “Search for boosted low-mass resonances decaying into hadrons produced in association with a photon”, *JHEP* **01** (2025) 099.

[8] ATLAS Collaboration, “Reinterpretation of searches for flavour-violating supersymmetry into flavour-violating dark-matter models”, ATL-PHYS-PUB-2025-010 (2025).

[9] C. G. Lester and D. J. Summers, “Measuring masses of semi-invisibly decaying particles pair-produced at hadron colliders”, *Phys. Lett. B* **463** (1999) 99.

[10] ATLAS Collaboration, “Search for new physics in final states with semi-visible jets or anomalous signatures”, *Phys. Rev. D* **112** (2025) 012021.

[11] ATLAS Collaboration, “Performance of missing transverse momentum reconstruction with the ATLAS detector using proton–proton collisions at $\sqrt{s}$ = 13 TeV”, *Eur. Phys. J. C* **78** (2018) 903,

[12] P. T. Komiske, E. M. Metodiev and J. Thaler, “Energy Flow Networks: Deep Sets for Particle Jets”, *JHEP* **01** (2019) 121.

[13] G. Matos, E. Busch, K. R. Park and J. Gonski, “Semi-supervised permutation invariant particle-level anomaly detection”, *JHEP* **05** (2025) 116.

[14] M. J. Strassler and K. M. Zurek, “Echoes of a hidden valley at hadron colliders”, *Phys. Lett. B* **651** (2007) 374.

[15] T. Han, Z. Si, K. M. Zurek and M. J. Strassler, “Phenomenology of hidden valleys at hadron colliders”, *JHEP* **07** (2008) 008.

PoS(EPS-HEP2025)418